

# Unbound excited states in $^{19,17}\text{C}$

Y. Satou<sup>a</sup>, T. Nakamura<sup>a</sup>, N. Fukuda<sup>b</sup>, T. Sugimoto<sup>b</sup>,  
Y. Kondo<sup>b</sup>, N. Matsui<sup>a</sup>, Y. Hashimoto<sup>a</sup>, T. Nakabayashi<sup>a</sup>,  
T. Okumura<sup>a</sup>, M. Shinohara<sup>a</sup>, T. Motobayashi<sup>b</sup>,  
Y. Yanagisawa<sup>b</sup>, N. Aoi<sup>b</sup>, S. Takeuchi<sup>b</sup>, T. Gomi<sup>b</sup>,  
Y. Togano<sup>c</sup>, S. Kawai<sup>c</sup>, H. Sakurai<sup>b</sup>, H. J. Ong<sup>d</sup>,  
T. K. Onishi<sup>d</sup>, S. Shimoura<sup>e</sup>, M. Tamaki<sup>e</sup>, T. Kobayashi<sup>f</sup>,  
H. Otsu<sup>b</sup>, Y. Matsuda<sup>f</sup>, N. Endo<sup>f</sup>, M. Kitayama<sup>f</sup>,  
and M. Ishihara<sup>b</sup>

<sup>a</sup>*Department of Physics, Tokyo Institute of Technology, 2-12-1 Oh-Okayama,  
Meguro, Tokyo 152-8551, Japan*

<sup>b</sup>*The Institute of Physical and Chemical Research (RIKEN), 2-1 Hirosawa, Wako,  
Saitama 351-0198, Japan*

<sup>c</sup>*Department of Physics, Rikkyo University, 3 Nishi-Ikebukuro, Toshima, Tokyo  
171-8501, Japan*

<sup>d</sup>*Department of Physics, University of Tokyo, 7-3-1 Hongo, Bunkyo, Tokyo  
113-0033, Japan*

<sup>e</sup>*Center for Nuclear Study (CNS), University of Tokyo, 2-1 Hirosawa, Wako,  
Saitama 351-0198, Japan*

<sup>f</sup>*Department of Physics, Tohoku University, Aoba, Sendai, Miyagi 980-8578,  
Japan*

---

**Abstract**

The neutron-rich carbon isotopes  $^{19,17}\text{C}$  have been investigated via proton inelastic scattering on a liquid hydrogen target at 70 MeV/nucleon. The invariant mass method in inverse kinematics was employed to reconstruct the energy spectrum, in which fast neutrons and charged fragments were detected in coincidence using a neutron hodoscope and a dipole magnet system. A peak has been observed with an excitation energy of 1.46(10) MeV in  $^{19}\text{C}$ , while three peaks with energies of 2.20(3), 3.05(3), and 6.13(9) MeV have been observed in  $^{17}\text{C}$ . Deduced cross sections are compared with microscopic DWBA calculations based on  $p$ - $sd$  shell model wave functions and modern nucleon-nucleus optical potentials.  $J^\pi$  assignments are made for the four observed states as well as the ground states of both nuclei.

*Key words:*

*PACS:* 24.10.-i, 25.40.Ep, 27.20.+n, 21.60.Cs

---

With the advent of new radioactive beam facilities capable of producing intense beams of various nuclear species far from the stability line, even at the drip-line, an increasingly large amount of information on nuclear levels and modes of excitation is being accumulated throughout the nuclear chart. New phenomena, such as nuclear halos and skins [1], enhanced  $E1$  transition strengths [2,3], and modifications of shell closures [4,5] have been revealed. Of particular interest in recent years are the neutron-rich carbon isotopes, which have attracted attention not only from their own structural interest, such as the anomalously reduced  $E2$  transition strength in  $^{16}\text{C}$  [6,7], but also for their implications for a new magic number at the neutron number  $N=16$  proposed in oxygen isotopes [5,8].

---

*Email address:* `satou@phys.titech.ac.jp` (Y. Satou).

Neutron number dependence of ground state deformations of carbon isotopes has been investigated in a deformed Hartree-Fock (HF) theory [9]. Generally the prolate deformation is expected at the beginning of the shell whereas oblate deformation arises towards the end of the shell. Note that the occurrence of nuclear deformations in the ground state is a consequence of the spontaneous symmetry breaking effect known in many fields of physics, and there is broad interest in elucidating the intriguing deformation-driving mechanism in atomic nuclei [10], which would be a nuclear physics analogue of the Jahn-Teller effect in molecular physics [11]. The theory predicts prolate deformations for carbon isotopes with  $N=9-11$ . For  $^{19}\text{C}$  with  $N=13$  two almost degenerate deformed minima are predicted with spins  $J^\pi=1/2^+$  (prolate) and  $3/2^+$  (oblate). Since the shape change at a neutron number smaller than the middle of  $N=8$  and  $20$  indicates a new shell closure at  $N=16$ , it is argued that definite information on the structure of  $^{19}\text{C}$  is important to clarify the possible new shell effect in the neutron-rich carbon isotopes [9,12].

The  $^{19}\text{C}$  nucleus is the heaviest odd carbon isotope. It is loosely bound with a neutron separation energy of  $S_n=0.58(9)$  MeV [13], and exhibits one-neutron halo structure as evidenced by large Coulomb break-up cross sections [14]. The ground state spin and parity were also investigated via the measurements of longitudinal momentum distributions of charged fragments after the removal of one neutron from  $^{19}\text{C}$  [15,16]. From these measurements the spin-parity was assigned to be  $J_{\text{g.s.}}^\pi=1/2^+$ . Other possibilities, however, have been suggested by authors in Ref. [17] based on their experiment in search of an isomeric transition. Moreover, there remains a controversy over the different widths of longitudinal momentum distributions measured at different energies [18,19], which has led to a conjecture of a possible resonance state just above the

particle decay threshold as a clue to solve such an inconsistency [20].

In this situation it is worthwhile accumulating experimental information on the ground as well as excited states of  $^{19}\text{C}$ . This paper reports a new measurement using the  $(p, p')$  inelastic scattering on  $^{19}\text{C}$  employing the invariant mass method in inverse kinematics. Both decaying neutrons and charged fragments were detected, and an isolated level was identified in the final state. The measurement was also made, partly for calibration purposes, on another loosely bound nucleus  $^{17}\text{C}$ , having  $S_n=0.73(2)$  MeV [13], for which  $J_{\text{g.s.}}^\pi$  is consistently reported to be  $3/2^+$  [16,21,22,23].

The  $(p, p')$  reaction has the following advantages: (1) The magnitude of the cross section, being sensitive to both the initial and final state wave functions, is configuration dependent. (2) The shape of the angular distribution also depends on the configuration through characteristic transferred  $L$  dependences of partial amplitudes. (3) Theoretical methods such as the distorted-wave Born approximation (DWBA) can be used to provide a first interpretation of data. There exists one  $(p, p')$  work on  $^{19}\text{C}$  reporting two bound states at 0.20 and 0.27 MeV using  $\gamma$ -ray spectroscopy [24]. These states are tentatively assigned as  $3/2^+$  and  $5/2^+$ , respectively, based on the assumption of  $J_{\text{g.s.}}^\pi=1/2^+$ . Close proximity of levels near the ground state has made it difficult to identify levels from comparisons in excitation energy between theory and experiment. Note that in shell model calculations [16] the triplet of levels are predicted below 0.62 MeV with no ground state configuration favoured. We have chosen to probe states in the unbound region, where in contrast to the bound region a lower level density is predicted up to about 3 MeV from the threshold in a shell model calculation described later. With no states known above the particle decay threshold, the measurement involved a search for resonances in

this region, and we report a new state in this paper. For  $^{17}\text{C}$  eleven new states up to 16.3 MeV excitation energy have been recently reported from the three-neutron transfer reaction  $^{14}\text{C}(^{12}\text{C}, ^9\text{C})^{17}\text{C}$ , with limited spin assignments [25]. This nucleus is also known to have a low-lying triplet of levels  $1/2^+$ ,  $3/2^+$ , and  $5/2^+$  below 0.33 MeV [24].

The experiment was performed at the RIKEN Accelerator Research Facility (RARF). The radioactive beams of  $^{19}\text{C}$  and  $^{17}\text{C}$  at 70 MeV/nucleon were produced using the projectile-fragment separator, RIPS [26], from a  $^{22}\text{Ne}$  primary beam at 110 MeV/nucleon. Typical beam intensities were 260 cps for  $^{19}\text{C}$  and 10.4 kcps for  $^{17}\text{C}$  with momentum spreads  $\Delta P/P$  of 3.0% and 0.1%, respectively. The secondary target was a cryogenic hydrogen target [27] having a cylindrical shape, 3 cm in diameter and  $120\pm 2$  mg/cm<sup>2</sup> in thickness. The target was surrounded by forty-eight NaI(Tl) scintillators used to detect de-excitation  $\gamma$ -rays from the charged fragments. Each crystal had a dimension of  $6.1\times 6.1\times 12.2$  cm<sup>3</sup>. The charged fragments were bent by a dipole magnet behind the target and were detected by a plastic counter hodoscope. Multi-wire drift chambers placed before and after the magnet were used to extract trajectory information of the charged particles. Neutrons were detected by a neutron hodoscope consisting of two walls of a plastic scintillator array placed 4.6 and 5.8 m behind the target. Each wall had a dimension of  $2.14^{\text{W}}\times 0.72^{\text{H}}$  (or  $0.90^{\text{H}}\times 0.12^{\text{T}}$ ) m<sup>3</sup>. The total efficiency of the hodoscope was  $24.1\pm 0.8\%$  for a threshold setting of 4 MeVee. This was deduced by measuring the  $^7\text{Li}(p, n)^7\text{Be}(\text{g.s.}+0.43\text{ MeV})$  reaction at  $E_p=70$  MeV and using existing cross section data [28]. The invariant mass of the final system was calculated event-by-event from the momentum vectors of the charged particle and the neutron. A series of studies probing unbound resonance states in beryllium

isotopes has been successfully performed using a detector setup similar to the present one [29,30,31].

Figure 1 shows relative energy spectra for the (a)  $^1\text{H}(^{19}\text{C}, ^{18}\text{C}+n)$ , (b)  $^1\text{H}(^{17}\text{C}, ^{16}\text{C}+n)$ , and (c)  $^1\text{H}(^{19}\text{C}, ^{16}\text{C}(2^+; 1.77 \text{ MeV})+n)$  reactions, integrated over center-of-mass angles up to  $\theta_{\text{c.m.}}=64^\circ$ . The effect of the finite detector acceptance was corrected for in panels (a) and (b), i.e. in inelastic channels. Shown in the insets of panels (a) and (b) are spectra obtained in coincidence with de-excitation  $\gamma$ -rays from the first  $2^+$  states at 1.58(1) MeV in  $^{18}\text{C}$  [32] and at 1.77(1) MeV in  $^{16}\text{C}$  [33], respectively. The spectrum in panel (c) also required the coincidence detection of  $\gamma$ -rays from the  $2^+$  state in  $^{16}\text{C}$ . Background contributions from various window materials surrounding the target, measured with an empty target, are subtracted. Error bars represent statistical uncertainties. Peak structures at about 0.9 MeV in relative energy in  $^{19}\text{C}$  and about 1.5 MeV in  $^{17}\text{C}$  are clearly seen in spectra without requiring  $\gamma$ -ray coincidences. They are absent in the respective  $\gamma$ -ray coincidence spectra. We thus conclude that charged particles resulting from the decay of these peaks are in their ground states. In panel (b) we can see two more peaks at about 0.6 and 3.6 MeV in relative energy. These are visible in the  $\gamma$ -ray coincidence spectrum in the inset of panel (b); the 0.6 MeV peak is more clearly populated in the spectrum in panel (c). This observation indicates that these peaks in  $^{17}\text{C}$  decay through the first  $2^+$  state in  $^{16}\text{C}$ .

The experimental spectra were analyzed to extract the resonance energy  $E_r$  and the width  $\Gamma_r$  in the following way. Firstly, a single Breit-Wigner shape function was generated for certain values of  $E_r$  and  $\Gamma_r$ :

$$\sigma(E_{\text{rel}}) \sim \frac{\Gamma_l(E_{\text{rel}})\Gamma_r}{\{E_r + \Delta E_l(E_{\text{rel}}) - E_{\text{rel}}\}^2 + \{\Gamma_l(E_{\text{rel}})/2\}^2}. \quad (1)$$

The shift function  $\Delta E_l(E_{\text{rel}})$  and the level width  $\Gamma_l(E_{\text{rel}})$ , which depend on the relative energy  $E_{\text{rel}}$ , were calculated by using the penetration  $P_l$  and shift  $S_l$  factors [34] by the relations:

$$\Delta E_l(E_{\text{rel}}) = \Gamma_r \times \{S_l(E_r) - S_l(E_{\text{rel}})\} / \{2P_l(E_r)\}, \quad (2)$$

$$\Gamma_l(E_{\text{rel}}) = \Gamma_r \times P_l(E_{\text{rel}}) / P_l(E_r), \quad (3)$$

where  $l$  refers to the decay angular momentum. Decay neutrons were supposed to be in the  $l=2$  orbit. The channel radius was taken to be  $R=r_0(A_n^{1/3} + A_f^{1/3})$  with  $r_0=1.4$  fm, where  $A_n$  and  $A_f$  are the neutron and charged fragment mass numbers, respectively. Then, the experimental resolution, including the detector resolution, beam profile, Coulomb multiple scattering of charged particles, and their range difference in the secondary target, was incorporated to generate a response function. The relative energy resolution was well simulated by  $\Delta E_{\text{rel}}=0.13\sqrt{E_{\text{rel}}}$  MeV (rms). The procedure was repeated for each resonance peak by varying the initial values of  $E_r$  and  $\Gamma_r$ . Parameters which gave the best fit to the data were obtained by minimizing the  $\chi^2$ . The solid curves in Fig. 1 show the results of the fit; the dashed lines background introduced to reproduce the overall spectrum.

Resonance parameters extracted are summarized in Table 1. The excitation energy  $E_x$  is obtained by the relation:  $E_x=E_r+S_n+E^*$ , where  $E^*$  refers to the excitation energy of the daughter nucleus. The state at  $E_x=1.46(10)$  MeV in  $^{19}\text{C}$  was observed for the first time in this measurement. The 2.20(3), 3.05(3), and 6.13(9) MeV states in  $^{17}\text{C}$  are respectively close to the 2.06, 3.10, and 6.20 MeV states observed in the three-neutron transfer reaction [25]. Extracted widths for the 1.46 and 2.20 MeV states are  $\Gamma_r=0.29(2)$  and  $0.53(4)$  MeV, respectively. These values are of the order of the respective single-particle

estimates for the width of  $l=2$  resonances [35],  $\Gamma_{\text{sp}}=0.25$  and  $0.78$  MeV, supporting the assumption of  $l=2$  decays of these states. For the  $3.05$  MeV state the  $\Gamma_r$  value was not extracted since it was insensitive to the spectrum shape owing to the very small penetration factors at low relative energies. Cross sections leading to these states, angle-integrated up to  $\theta_{\text{c.m.}}=64^\circ$ , are given in Table 1. Differential cross sections leading to the  $1.46$  MeV state in  $^{19}\text{C}$  are shown in Fig. 2, and those to the  $2.20$  and  $3.05$  MeV states in  $^{17}\text{C}$  are shown in Fig. 3. The errors shown are the quadratic sum of statistical and systematic uncertainties; the latter in the absolute magnitude of the cross section is estimated to be  $7\%$ , including ambiguities in target thickness, neutron detection efficiency, and fitting procedure. The angular resolution varied from  $\Delta\theta_{\text{c.m.}}=3.4^\circ$  ( $3.1^\circ$ ) in rms at  $\theta_{\text{c.m.}}=4^\circ$  to  $5.1^\circ$  ( $4.6^\circ$ ) at  $60^\circ$  for  $^{19}\text{C}$  ( $^{17}\text{C}$ ).

To obtain an understanding of the results shell model calculations were performed using the code OXBASH [36] within the  $0\hbar\omega$  configurations in the  $p$ - $sd$  shell model space. For  $^{19}\text{C}$ , the second  $5/2_2^+$  state is predicted at  $1.40$ ,  $1.54$ , and  $1.47$  MeV with the WBT, WBP [37], and MK [38] interactions, respectively. These energies are close to the experimental value of  $1.46$  MeV; it is likely that this state corresponds to the  $5/2_2^+$  state. The closest higher-lying state is the  $7/2_1^+$  state predicted  $0.7$ – $1.0$  MeV above the  $5/2_2^+$  state. For  $^{17}\text{C}$ , with the WBT interaction four states  $5/2_2^+$  ( $1.72$  MeV),  $7/2_1^+$  ( $2.33$  MeV),  $9/2_1^+$  ( $3.01$  MeV), and  $3/2_2^+$  ( $3.08$  MeV) are predicted above the decay threshold and below  $3.5$  MeV.

In order to further clarify the nature of states involved in transitions shown in Table 1, microscopic DWBA calculations were performed using the code DW81 [39]. The optical potential was taken from the global parameterization KD02 [40]. A microscopic optical potential [41] based on the approach of



Jeukenne, Lejeune, and Mahaux (JLM) [42] was also tested. The projectile-nucleon effective interaction was the M3Y interaction [43]. The transition density was calculated with the shell model using the WBT interaction [37]. The single-particle wave function was generated in a harmonic oscillator well. The oscillator parameter was chosen so that the rms radius corresponding to the wave function reproduces the experimental value [44]:  $b=2.07$  fm for  $^{19}\text{C}$  and  $1.83$  fm for  $^{17}\text{C}$ . The effect of core polarization on quadrupole transition amplitudes was taken into account in the isoscaler channel, by introducing isospin dependent polarization charges obtained in the FH+RPA particle-vibration model and parameterized in Ref. [10]:  $\delta_{T=0}=0.17$  for  $^{19}\text{C}$  and  $0.22$  for  $^{17}\text{C}$ . Integrated DWBA cross sections are given in Table 1 for each transition listed. The  $J^\pi$  values are discussed below.

In Fig. 2, the DWBA predictions of the differential cross section leading to the  $1.46$  MeV state in  $^{19}\text{C}$  are shown for three possible ground-state configurations. The solid line was obtained by using the KD02 optical potential for the supposed  $1/2_1^+ \rightarrow 5/2_2^+$  transition, while the dot-dashed line by using the JLM potential for the same transition. The latter was specifically derived for the  $p+^{19}\text{C}$  system at  $E_p=70$  MeV. These curves agree closely with each other, justifying an extrapolated use in mass number of the KD02 potential (the nominal range is  $A=27-209$ ) down to the  $A=19$  region even for nuclei with large neutron/proton ratios. We therefore adopt the KD02 potential below. Dashed and dotted curves respectively assume  $J_{\text{g.s.}}^\pi=3/2_1^+$  and  $5/2_1^+$ , and the same final state. These curves fail to reproduce the magnitude of the cross section. Clearly, the data are much better described by the solid and dot-dashed curves obtained with  $J_{\text{g.s.}}^\pi=1/2_1^+$ . If the  $1.46$  MeV levels is not  $5/2_2^+$ , it might be identified with the  $7/2_1^+$  state. DWBA cross sections exciting this

$7/2_1^+$  state from any of the members of the low-lying triplet, integrated up to  $\theta_{\text{c.m.}}=64^\circ$ , are, however, at most 4.2 mb (for  $5/2_1^+ \rightarrow 7/2_1^+$ ), only 50% of the data. We thus conclude that the spin of the ground state of  $^{19}\text{C}$  is consistent with  $J^\pi=1/2^+$  [14,15,16], and that of the 1.46 MeV state is  $5/2^+$ .

In the study of the  $^{14}\text{C}(^{12}\text{C},^9\text{C})^{17}\text{C}$  reaction [25], a state was observed at 2.06 MeV in  $^{17}\text{C}$ , which was assigned as either  $3/2_2^+$  or  $7/2_1^+$  using the results of shell model calculations. Although there is a slight discrepancy in the excitation energies, a possible counterpart of this state is the 2.20 MeV state in the present  $(p, p')$  study, for which we examine the two proposed  $J^\pi$  assignments. Of all possible transitions connecting the low-lying triplet of states and the  $(3/2_2^+, 7/2_1^+)$  state, it is found that only three have sizeable cross sections when integrated up to  $\theta_{\text{c.m.}}=64^\circ$ : 2.3 mb for  $1/2_1^+ \rightarrow 3/2_2^+$ , 2.7 mb for  $3/2_1^+ \rightarrow 7/2_1^+$ , and 3.0 mb for  $5/2_1^+ \rightarrow 7/2_1^+$ . The DWBA cross sections for other transitions are at most 0.66 mb ( $3/2_1^+ \rightarrow 3/2_2^+$ ). Of the three the  $1/2_1^+ \rightarrow 3/2_2^+$  case is readily excluded since it has been clearly demonstrated in a  $g$ -factor measurement that  $J_{\text{g.s.}}^\pi$  of  $^{17}\text{C}$  is different from  $1/2^+$  [21]. We are thus left with the  $7/2_1^+$  assignment for the 2.20 MeV state. DWBA predictions leading to this state are shown in Fig. 3 for three initial-state configurations: solid line assumes  $J_{\text{g.s.}}^\pi=3/2_1^+$ , dashed one  $5/2_1^+$ , and dotted one  $1/2_1^+$ . The  $1/2_1^+ \rightarrow 7/2_1^+$  assumption gives much lower cross sections than the data. Of the remaining two we see that the  $3/2_1^+$  assumption for the ground state better describes the data by reproducing the slope of the angular distribution, although the  $5/2_1^+$  assumption also gives a reasonable description of the data.

In Fig. 3, differential cross sections leading to the 3.05 MeV state are also compared with DWBA predictions obtained by assuming different configurations for the ground state, and the  $9/2_1^+$  state for the excited state. This state

was populated only weakly. It had a sizeable cross section only at backward angles, where transition amplitudes with large angular momentum transfers are involved. It could be identified as the  $9/2^+$  state reported at 3.10 MeV in the three-neutron transfer work [25], and predicted at 3.01 MeV in the present shell model calculations. The cross sections leading to this state are in good agreement with the solid curve calculated for the  $3/2_1^+ \rightarrow 9/2_1^+$  transition, excluding the possibility of  $J_{\text{g.s.}}^\pi = 5/2_1^+$  for  $^{17}\text{C}$ . This further corroborates the earlier  $3/2^+$  assignments for the ground state of this nucleus [16,21,22,23], giving us confidence in the current procedure employing the shell model wave functions and DWBA calculations.

The 6.13 MeV state in  $^{17}\text{C}$  appears to correspond to the 6.20 MeV state reported close in energy in the three-neutron transfer work [25]. In that study it was tentatively assigned as either  $5/2_4^+$  or  $5/2_5^+$ , with a preference for the latter assignment due to larger occupancies predicted for the  $0d$  shells. The  $5/2_4^+$  and  $5/2_5^+$  states are located at 6.25 and 6.81 MeV, respectively, in the present shell model calculations using the WBT interaction. DWBA cross sections leading to the  $5/2_4^+$  and  $5/2_5^+$  states, angle integrated up to  $\theta_{\text{c.m.}} = 64^\circ$ , are 0.94 and 0.25 mb, respectively. The experimental value of 0.8(1) mb favours the  $5/2_4^+$  assignment for this state. The  $5/2_4^+$  state is predicted to have a large occupancy of the  $0d3/2$  shell of 23%, which corresponds to almost one neutron in this shell, in contrast to other lower energy states involved in this study: 4%, 4%, and 6% for the ground,  $7/2_1^+$ , and  $9/2_1^+$  states, respectively. This indicates that promoting one neutron from lower-lying shells to the  $0d3/2$  shell is the dominant excitation process of this state. The deduced narrow width is consistent with the reported value of  $\Gamma_r = 0.35(15)$  MeV in Ref. [25].

The  $5/2_2^+$  shell model state at 1.72 MeV in  $^{17}\text{C}$  is not observed clearly pre-

sumably due to the large expected width [25]. The angle integrated DWBA cross section leading to this state from the  $3/2_1^+$  ground state was calculated to be 0.69 mb.

According to the argument of Ref. [9] the spin of  $J_{\text{g.s.}}^\pi=1/2_1^+$  for  $^{19}\text{C}$  may imply a prolate intrinsic deformation for the ground state. In terms of the Nilsson diagram this indicates that four neutrons occupy the  $[220\frac{1}{2}]$  and  $[211\frac{3}{2}]$  orbits, and one neutron occupies the  $[211\frac{1}{2}]$  orbit in the ground state, where  $[Nn_z\Lambda\Omega]$  are asymptotic quantum numbers referring to large prolate deformations. If one assumes that the observed  $1/2^+ \rightarrow 5/2^+$  transition is primarily associated with the promotion of the least bound neutron in the  $[211\frac{1}{2}]$  orbit to the  $[202\frac{5}{2}]$  orbit, one would obtain a value for the quadrupole deformation parameter of  $\beta_2 \approx 0.4$ , by referring to neutron single-particle levels in a deformed Woods-Saxon potential [45], and by equating the excitation energy of 1.46 MeV with the energy difference of the two Nilsson orbits. Interestingly, this value is consistent with the result of more recent deformed Skyrme HF calculations predicting a local prolate minimum with  $J^\pi=1/2^+$  at  $\beta_2=0.39$  [10]. In the HF calculation, however, the ground state was predicted to be oblate with  $\beta_2=-0.36$  and  $J^\pi=3/2^+$ , and to be more bound by 2.05 MeV than the prolate minimum. Moreover a local oblate minimum having  $J^\pi=1/2^+$  with  $\beta_2=-0.35$  was also predicted to be almost degenerate with the  $J^\pi=3/2^+$  ground state. The present cross section for the  $1/2^+ \rightarrow 5/2^+$  transition observed in  $^{19}\text{C}$  will be useful in distinguishing between the two  $1/2^+$  states with different signs of  $\beta_2$ , and provide a clue to further investigate the persistence of the new magic number  $N=16$  proposed in oxygen isotopes [5,8] down to the carbon isotopes. The HF model [10] gives a good account of the ground state spin of  $3/2^+$  for  $^{17}\text{C}$ . It is of interest to see if it also accounts for other states observed in this

experiment.

In summary, we have demonstrated that the  $(p, p')$  reaction using the invariant mass method in inverse kinematics leading to unbound resonance states in the residual nucleus is feasible for structure studies even for nuclei far from stability. The measurements were made on  $^{19,17}\text{C}$  at 70 MeV/nucleon. One resonance in  $^{19}\text{C}$  and three in  $^{17}\text{C}$  were observed above the particle decay threshold. A DWBA analysis employing shell model wave functions and modern nucleon-nucleus optical potentials was used to identify the transitions observed. The spin-parity of the ground state of  $^{19}\text{C}$  was found to be consistent with  $1/2^+$ , and that of the strongly excited 1.46 MeV state was assigned to be  $5/2_2^+$ . For  $^{17}\text{C}$  the observed states corresponded well with those reported in a three-neutron transfer study [25]. By adding information from this experiment spin-parity assignments of  $7/2_1^+$  for the 2.20 MeV state and  $5/2_4^+$  for the 6.13 MeV state were made. The spectroscopic information from this study will impose stringent constraints on further theoretical investigations of light neutron-rich nuclei in this region.

The authors acknowledge invaluable assistance of the staff of RARF during the experiment, particularly, Dr. Y. Yano, Dr. A. Goto, and Dr. M. Kase, and useful discussions with Professor I. Hamamoto and Professor J. A. Tostevin. This work was supported, in part, by the Grant-in-Aid for Scientific Research (Nos. 15540257 and 15740145) from MEXT Japan.

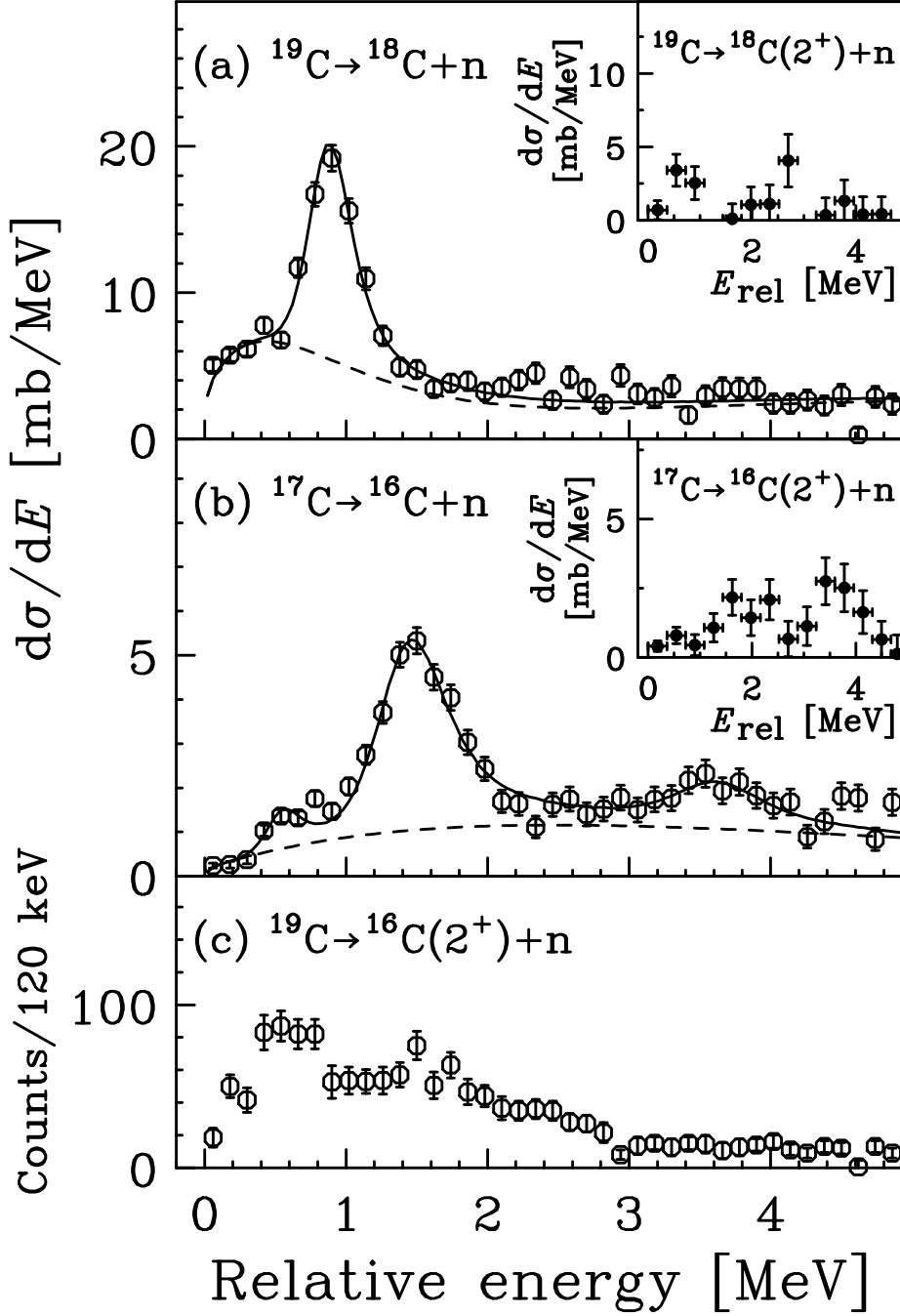


Fig. 1. Relative energy spectra integrated over an angular range below  $\theta_{\text{c.m.}} = 64^\circ$  for the (a)  $^1\text{H}(^{19}\text{C}, ^{18}\text{C} + n)$ , (b)  $^1\text{H}(^{17}\text{C}, ^{16}\text{C} + n)$ , and (c)  $^1\text{H}(^{19}\text{C}, ^{16}\text{C}(2^+; 1.77 \text{ MeV}) + n)$  reactions at 70 MeV/nucleon. Shown in the insets of panels (a) and (b) are spectra obtained in coincidence with de-excitation  $\gamma$ -rays from the first  $2^+$  states of the respective charged fragments. The instrumental background was subtracted in the spectra. Solid lines represent the results of the fit, dashed lines background introduced to reproduce the overall spectrum.

Table 1

Resonance parameters and populating cross sections from this experiment. The excitation energy and the cross section are compared to theoretical values. Cross sections are integrated up to  $\theta_{\text{c.m.}}=64^\circ$ . DWBA cross sections  $\sigma_{\text{DWBA}}$  leading to states specified by  $J^\pi$  are obtained by using the shell model wave functions with the WBT interaction, assuming  $J_{\text{g.s.}}^\pi=1/2_1^+$  for  $^{19}\text{C}$  and  $3/2_1^+$  for  $^{17}\text{C}$ .

Nucleus	Experiment				Theory		
	$E_r$	$E_x$	$\Gamma_r$	$\sigma_{\text{exp}}$	$E_x$	$\sigma_{\text{DWBA}}$	$J^\pi$
	(MeV)	(MeV)	(MeV)	(mb)	(MeV)	(mb)	
$^{19}\text{C}$	0.88(1)	1.46(10)	0.29(2)	8.6(4)	1.40	6.9	$5/2_2^+$
$^{17}\text{C}$	1.47(2)	2.20(3)	0.53(4)	3.8(2)	2.33	2.7	$7/2_1^+$
	0.55(2)	3.05(3)	—	0.40(4)	3.01	0.48	$9/2_1^+$
	3.63(9)	6.13(9)	$0.26^{+0.4}_{-0.26}$	0.8(1)	6.25	0.94	$5/2_4^+$

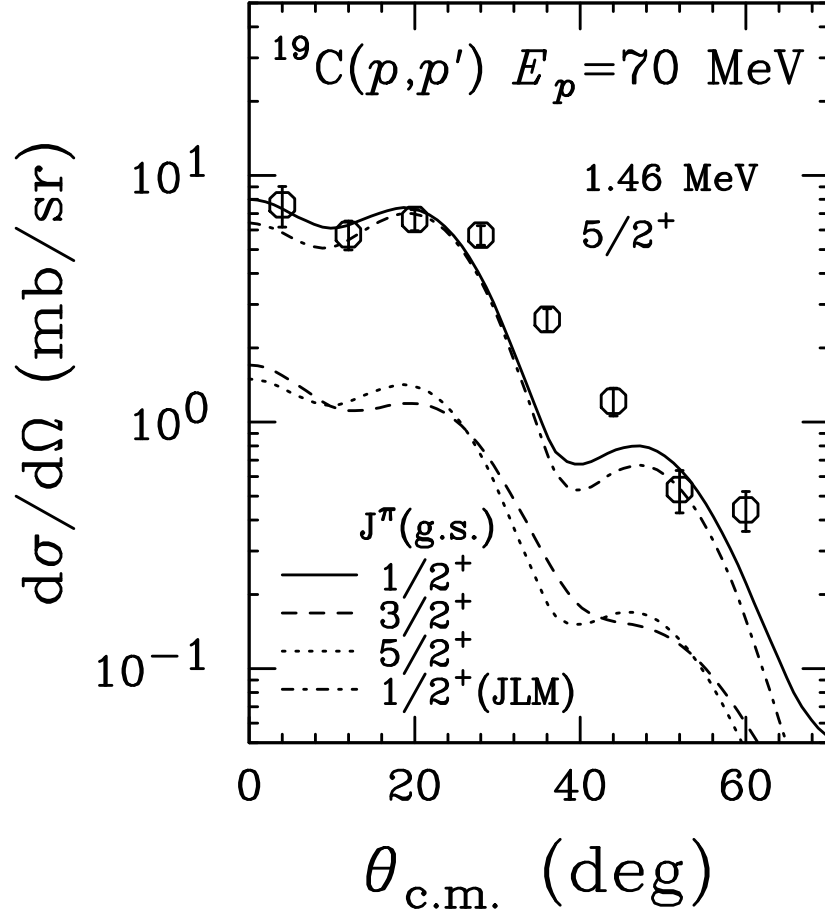


Fig. 2. Differential cross sections leading to the 1.46 MeV state in  $^{19}\text{C}$  are compared to DWBA predictions obtained by assuming different initial-state configurations.  $J^\pi=5/2_2^+$  is assumed for the excited state.



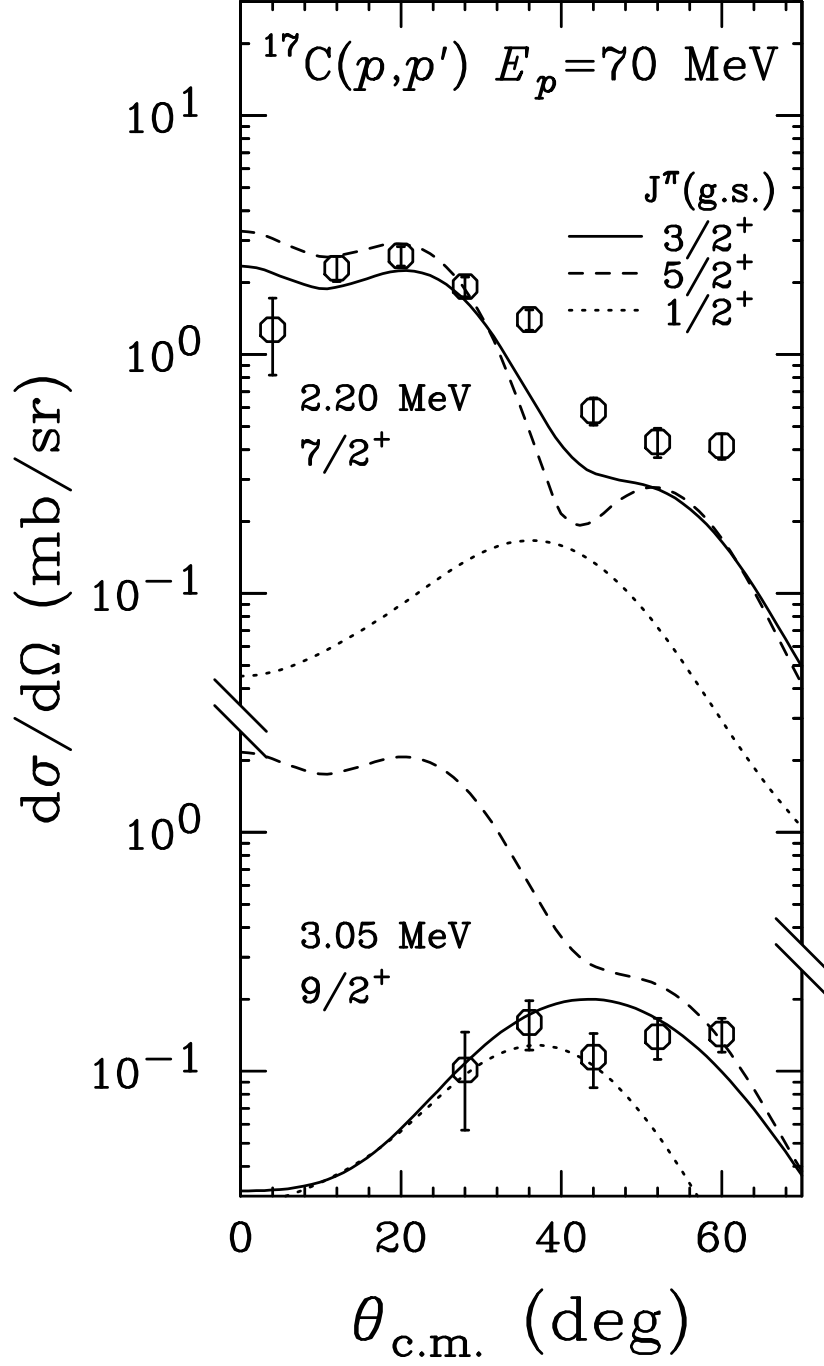


Fig. 3. Differential cross sections leading to the 2.20 and 3.05 MeV states in  $^{17}\text{C}$  are compared to DWBA predictions obtained by assuming different initial-state configurations.  $J^\pi$  values assumed for the excited states are  $7/2_1^+$  and  $9/2_1^+$  for the 2.20 and 3.05 MeV states, respectively.

## References

- [1] I. Tanihata *et al.*, Phys. Rev. Lett. **55**, 2676 (1985).
- [2] T. Nakamura *et al.*, Phys. Lett. B **331**, 296 (1994); Phys. Rev. Lett. **96**, 252502 (2006).
- [3] P. Adrich *et al.*, Phys. Rev. Lett. **95**, 132501 (2005).
- [4] H. Iwasaki *et al.*, Phys. Lett. B **481**, 7 (2000).
- [5] A. Ozawa *et al.*, Phys. Rev. Lett. **84**, 5493 (2000).
- [6] N. Imai *et al.*, Phys. Rev. Lett. **92**, 062501 (2004).
- [7] Z. Elekes *et al.*, Phys. Lett. B **586**, 34 (2004).
- [8] Z. Elekes *et al.*, Phys. Rev. Lett. **98**, 102502 (2007).
- [9] T. Suzuki *et al.*, in the *Proceedings of the International Symposium on Frontiers of Collective Motions (CM2002)*, edited by H. Sagawa and H. Iwasaki (World Scientific, Singapore, 2003), p. 236.
- [10] H. Sagawa *et al.*, Phys. Rev. C **70**, 054316 (2004).
- [11] H. A. Jahn and E. Teller, Proc. R. Soc. London, Ser. A **161**, 220 (1937).
- [12] T. Suzuki *et al.*, Phys. Rev. C **68**, 014317 (2003).
- [13] G. Audi, A. H. Wapstra, and C. Thibault, Nucl. Phys. **A729**, 337 (2003).
- [14] T. Nakamura *et al.*, Phys. Rev. Lett. **83**, 1112 (1999).
- [15] D. Bazin *et al.*, Phys. Rev. Lett. **74**, 3569 (1995).
- [16] V. Maddalena *et al.*, Phys. Rev. C **63**, 024613 (2001).
- [17] R. Kanungo *et al.*, Nucl. Phys. **A757**, 315 (2005).

- [18] D. Bazin *et al.*, Phys. Rev. C **57**, 2156 (1998).
- [19] T. Baumann *et al.*, Phys. Lett. B **439**, 256 (1998).
- [20] M. H. Smedberg and M. V. Zhukov, Phys. Rev. C **59**, 2048 (1999).
- [21] H. Ogawa *et al.*, Eur. Phys. J. A **13**, 81 (2002).
- [22] E. Sauvan *et al.*, Phys. Lett. B **491**, 1 (2000); Phys. Rev. C **69**, 044603 (2004).
- [23] U. Datta Pramanik *et al.*, Phys. Lett. B **551**, 63 (2003).
- [24] Z. Elekes *et al.*, Phys. Lett. B **614**, 174 (2005).
- [25] H. G. Bohlen *et al.*, Eur. Phys. J. A **31**, 279 (2007).
- [26] T. Kubo, *et al.*, Nucl. Instrum. Methods Phys. Res. B **70**, 309 (1992).
- [27] H. Ryuto, *et al.*, Nucl. Instrum. Methods Phys. Res. A **555**, 1 (2006).
- [28] T. N. Taddeucci *et al.*, Phys. Rev. C **41**, 2548 (1990).
- [29] N. Fukuda *et al.*, Phys. Rev. C **70** 054606 (2004).
- [30] T. Sugimoto *et al.*, Phys. Lett. B **654**, 160 (2007).
- [31] Y. Kondo, Doctoral Dissertation, Tokyo Institute of Technology, (2007).
- [32] M. Stanoiu *et al.*, Eur. Phys. J. A **20**, 95 (2004).
- [33] D. R. Tilley, H. R. Weller, and C. M. Cheves, Nucl. Phys. **A564**, 1 (1993).
- [34] A. M. Lane and R. G. Thomas, Rev. Mod. Phys. **30**, 257 (1958).
- [35] A. Bohr and B. R. Mottelson, *Nuclear Structure* (Benjamin, New York, 1969),  
Vol. 1, p. 441.
- [36] The shell model code OXBASH, B. A. Brown *et al.*, *NSUCL Report* **524** (1988).
- [37] E. K. Warburton and B. A. Brown, Phys. Rev. C **46**, 923 (1992).

- [38] D. J. Millener and D. Kurath, Nucl. Phys. **A255**, 315 (1975).
- [39] Program DWBA70, R. Schaeffer and J. Raynal (unpublished); Extended version DW81, J. R. Comfort (unpublished).
- [40] A. J. Koning and J. P. Delaroche, Nucl. Phys. **A713**, 231 (2003).
- [41] A. García-Camacho, R. C. Johnson, and J. A. Tostevin, Phys. Rev. C **71**, 044606 (2005).
- [42] J. P. Jeukenne, A. Lejeune, and C. Mahaux, Phys. Rev. C **16**, 80 (1977).
- [43] G. Bertsch *et al.*, Nucl. Phys. **A284**, 399 (1977).
- [44] A. Ozawa, T. Suzuki, and I. Tanihata, Nucl. Phys. **A693**, 32 (2001).
- [45] I. Hamamoto, Phys. Rev. C **76**, 054319 (2007).